

# Nematohydrodynamic Effects on the Phase Separation of a Symmetric Mixture of an Isotropic Liquid and a Liquid Crystal

Takeaki Araki and Hajime Tanaka

*Institute of Industrial Science, University of Tokyo, Meguro-ku, Tokyo 153-8505, Japan*

(Received 23 January 2004; published 30 June 2004)

We numerically study phase-separation dynamics of symmetric mixtures of an isotropic liquid and a liquid crystal, incorporating nematohydrodynamics, for the first time. We find that the hydrodynamics not only accelerates the domain growth, but also leads to the breakdown of the morphological symmetry of the two phases, which occupy the same volume: The liquid-crystal-rich phase tends to form isolated domains. This symmetry breaking is revealed to be induced by the flow-alignment coupling due to the anisotropic shape of liquid crystal molecules (kinetic effects), and not by the elastic asymmetry (energetic effects).

DOI: 10.1103/PhysRevLett.93.015702

PACS numbers: 64.75.+g, 64.70.Md, 83.80.Xz, 47.54.+r

Phase-separation phenomena are widely observed in various kinds of condensed matter including metals, simple liquids, and complex fluids such as polymers, surfactants, and liquid crystals [1]. Their dynamics are often classified into “solid model” and “fluid model,” depending upon the transport mechanism of mixtures [1]. These models predict (a) morphological symmetry [2], which is characterized by the zero average mean curvature of the interface, and (b) self-similar growth for a symmetric mixture, for which the two coexisting phases occupy the same volume. Recently, however, two exceptions to this conventional wisdom have been found for isotropic mixtures. (i) Phase separation in solid mixtures with elastic misfit, where the harder phase forms isolated domains to reduce the total elastic energy [1]. (ii) Viscoelastic phase separation of dynamically asymmetric mixtures, where the volume of the more viscoelastic phase shrinks even after the formation of the sharp interface [3]. In this Letter, we report a novel mechanism of the purely kinetic origin, which leads to the breakdown of the morphological symmetry and the self-similar growth for a symmetric mixture of an isotropic liquid (IL) and a liquid crystal (LC).

The typical phase diagram of an IL-LC mixture, which is composed of the coexistence curve and the isotropic-nematic (IN) transition line, is shown in Fig. 1. In a certain region of the phase diagram, both compositional (phase separation) and orientational ordering (nematic ordering) take place simultaneously. This phenomenon has attracted considerable interest both technologically and scientifically [4–14]. For example, polymer-dispersed liquid crystals, which are produced by using phase-separation of polymers and liquid crystals, are widely applied for electro-optical devices. Theoretically, on the other hand, the phase-separation process is described by the coupled dynamics of the two order parameters, composition  $\phi$  and orientational order parameter  $Q$  [15], which is somewhat similar [4–10] to that of the so-called model C [1]. However, it also includes new features stemming from (a) the tensorial nature of  $Q$

[11–14] and (b) its peculiar hydrodynamics (nematohydrodynamics) [16–19]. Although effect (a) has been studied intensively, effect (b) has not been explored so far, despite that nematohydrodynamics is one of the most essential features of LC and should cause drastic effects on the phase-separation kinetics, as hydrodynamics does for binary fluid mixtures. It is the aim of this Letter to elucidate the effects of nematohydrodynamics on the phase-separation behavior of IL-LC mixtures.

First we describe the coarse-grained model of phase separation of IL-LC mixtures, which is used in our numerical simulations. Here we consider only the two-dimensional (2D) system for simplicity. We employ the Landau-type free energy for the mixing free energy:  $f_{\text{mix}}(\phi) = -\frac{1}{2}\phi^2 + \frac{1}{4}\phi^4$ . Here  $\phi = \pm 1$  represent the equilibrium concentrations unless the nematic ordering takes place;  $\phi > 0$  corresponds to the LC-rich phase. To describe the IN transition, on the other hand, we employ the following free energy for the orientational order:  $f_{LdG}(\phi, Q) = -\frac{1}{2}a(\phi)Q^2 + \frac{1}{4}Q^4$ . Here the nematic ordering is treated as the second-order phase transition, since it should be the case for 2D ( $d = 2$ ) [13]. In the above,  $a(\phi) = \frac{\phi - \phi^*}{1 - \phi^*}$ , where  $\phi^*$  is the threshold concentration, above which the nematic ordering takes place.

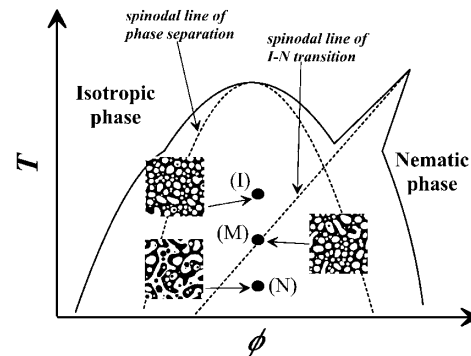


FIG. 1. Schematic phase diagram of an IL-LC mixture. Domain patterns of the symmetric mixture simulated for different quench depths are also drawn.

Thus, the total free-energy functional of the system is given as

$$\mathcal{F}\{\phi, Q_{ij}\} = \int dV \left[ f_{\text{mix}}(\phi) + \frac{1}{2} |\nabla \phi|^2 + w \partial_i \phi \partial_j \phi Q_{ij} + \alpha \left\{ f_{\text{LDG}}(\phi, Q_{ij}) + \frac{1}{2} \epsilon^2 (\partial_k Q_{ij})^2 \right\} \right]. \quad (1)$$

Here the free energy and the length are scaled by  $\sigma \xi^2$  and  $\xi$ , respectively.  $\sigma$  is the interface tension of the coexisting phases, and  $\xi$  is the correlation length of concentration fluctuations. The other parameters are defined as  $\alpha = \frac{K_F \xi}{\sigma \Xi^2}$ ,  $\epsilon = \frac{\Xi}{\xi}$ , and  $w = \frac{K_F}{\sigma l}$ , where  $K_F$  and  $\Xi$  are the Frank elastic constant and the correlation length of orientational fluctuations, respectively.  $l$  is the penetration length, which represents the effects of the anchoring of the director field to the interface. Here we note that in our model the quench condition is determined solely by the initial composition  $\phi_0$  and  $\phi^*$  (see Fig. 1).

Next we describe the dynamic equations for  $\phi$  and  $Q$ .

$$\frac{D}{Dt} \phi = \nabla^2 \mu + \delta \phi, \quad (2)$$

$$\frac{D}{Dt} Q_{ij} = \kappa_{ik}^a Q_{kj} - Q_{ik} \kappa_{kj}^a + L_2 H_{ij} + \beta \kappa_{ij}^s + \delta Q_{ij}, \quad (3)$$

where  $t$  is the time scaled by the characteristic diffusion time [20] and  $D/Dt$  is the Lagrange time derivative. Here  $\mu$  and  $H$  are the chemical potential and the molecular force field, respectively;  $\mu = \frac{\delta \mathcal{F}}{\delta \phi}$  and  $H = -\left(\frac{\delta \mathcal{F}}{\delta Q} - \frac{1}{d} \mathbf{I} \text{Tr} \frac{\delta \mathcal{F}}{\delta Q}\right)$ .  $\kappa_{ij}^s$  and  $\kappa_{ij}^a$  are the symmetric and asymmetric parts of the velocity gradient tensor  $\partial_i v_j$ , respectively. In the above kinetic equations, we set the off-diagonal Onsager kinetic coefficients between  $\phi$  and  $Q$  to be zero. This coupling between diffusion and rotation is important for polymeric LC [13,14], but negligible for low-molecular-weight LC, which we consider in this Letter.  $L_2 \alpha \alpha(\phi)$  is the scaled rotational rate.  $\beta$  is the so-called flow-alignment parameter, which represents the coupling between the director and the flow fields. The value of  $\beta$  is purely determined by a shape of the LC molecules. It is positive for usual rodlike LC, but negative for discotic LC. Note that  $\beta = 0$  for spherical molecules. Here we stress that  $\beta$  is the most essential kinetic coupling parameter characteristic of anisotropic LC molecules.

For the velocity field, we employ the quasistationary approximation. Thus the hydrodynamic equation is described as [17–19]

$$-\phi \partial_i \mu + \partial_j (H_{ik} Q_{kj} - Q_{ik} H_{kj}) + Q_{jk} \partial_i H_{kj} - \beta \partial_j H_{ij} - \partial_i p + \frac{1}{R} \nabla^2 v_i \approx 0. \quad (4)$$

Here  $R$  is the dimensionless universal parameter that is inversely proportional to the viscosity [20]. It is worth noting that the force  $Q_{jk} \partial_i H_{kj}$  is essentially the same as the force stemming from the Ericksen tensor of nematic

hydrodynamics [16]. For simplicity, the dependence of the viscosity on the orientational order is neglected.  $p$  is a part of pressure, which is determined to satisfy the incompressible condition  $\partial_i v_i = 0$ .

We numerically solve Eqs. (2) and (3) by using an explicit Euler scheme, in which the discretized space and time are  $\Delta x = 1.0$  and  $\Delta t = 0.01$ . We set  $\alpha = 0.2$ ,  $R = 10$ ,  $\epsilon = 0.4$ ,  $w = 0.1$ , and  $L_2 = 25$  [21]. We keep imposing the Gaussian noises, whose intensities are  $|\delta \phi| = 1 \times 10^{-4}$  and  $|\delta Q_{ij}| = 1 \times 10^{-4}$ , respectively, in Eqs. (2) and (3). Equation (4) is solved by the fast Fourier transform method [20].

First we show the simulated pattern evolution processes. Figure 2(a) shows the pattern evolution for case (A), where the hydrodynamic flow is neglected ( $R = 0$  and  $\beta = 0$ ). Figures 2(b) and 2(c), on the other hand, show those for case (B), where the hydrodynamics is included ( $R = 10$ ) but the kinetic coupling of flow and orientational fields is neglected ( $\beta = 0$ ), and case (C), where both are included ( $R = 10$  and  $\beta = 2$ ). For these simulations, we set  $\phi_0 = \phi^* = 0$ , which corresponds to point (M) in Fig. 1. Initial states of cases (A)–(C) are unstable with respect to phase separation and just marginal for nematic ordering. Thus the symmetric bicontinuous domain pattern emerges as in the ordinary symmetric binary fluid mixtures in the early stage of phase separation. Then the IN transition is induced selectively in the LC-rich phase ( $\phi > \phi^*$ ).

For cases (A) and (B), the self-similarity of the domain growth is observed; that is, the domain pattern evolves while keeping its symmetric bicontinuous structure, as seen in isotropic fluid mixtures. For case (A), the phase separation and nematic ordering proceed only via translational and rotational diffusion, respectively. Since we assume that the characteristic time scale of the rotation of

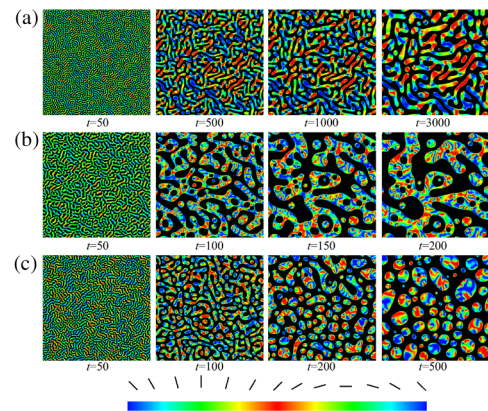


FIG. 2 (color online). Simulated phase-separation processes of the mixture of IL and LC. (a)  $R = 0$ ; (b)  $R = 10$  and  $\beta = 0$ ; (c)  $R = 10$  and  $\beta = 2$ . The black phase represents the IL-rich phase ( $\phi < 0$ ) and the color inside the LC-rich phase ( $\phi > 0$ ) represents the orientational field of the nematic phase, that is,  $Q_{xy}$ . The relationship between the orientation and the color is shown at the bottom.

LC molecules is shorter than that of the translational diffusion, the director field can catch up with the interface motion; the orientational order can quickly relax to reduce the elastic energy of the nematic phase, which is dominated by the anchoring to the interface. Thus, defects are rarely produced in the nematic phase [compare case (A) with case (B)]. We can say that the orientational field  $\mathbf{Q}$  behaves as the slave variable of the concentration  $\phi$  for case (A). For case (B), the domain growth is accelerated by hydrodynamic flow driven by the interface tension, which is included in the term  $-\phi\partial_i\mu$  of Eq. (4). Thus, the pattern evolution of case (B) is much faster than that of case (A). This is the usual hydrodynamic acceleration of domain coarsening [1,20]. We note that the flow caused by the elastic force,  $Q_{jk}\partial_i H_{kj}$ , does not affect the domain coarsening itself [18]. Thus, the orientational field cannot follow the accelerated interface motion, which results in the creation of many defects in the LC-rich phase.

For case (C), we also observe the symmetric bicontinuous structure in the very early stage ( $t \lesssim 50$ ), as seen in cases (A) and (B). When the hydrodynamic flow sets in, however, the nematic phase is disconnected selectively and, thus, the symmetric bicontinuous structure transforms into the nematic droplet one in the late stage ( $t \gtrsim 200$ ), despite the volume symmetry. As the result, the self-similarity of the domain coarsening is also broken. The only difference between case (B) and case (C) is the degree of the flow-alignment coupling. This suggests that the flow-alignment coupling is the physical origin of the morphological symmetry breaking [22]. The relevance of this scenario is checked below.

Figure 3 shows the temporal change in the averaged curvature of the interface for the mixtures of various  $\beta$  [the other parameters are the same as those of case (C)]. The curvature is calculated as  $h = -\nabla \cdot (\nabla\phi/|\nabla\phi|)$ . The almost zero ( $h \approx 0$ ) and positive ( $h > 0$ ) values correspond to the symmetric bicontinuous and nematic droplet structures, respectively. For the mixture without the flow-alignment coupling,  $\langle h \rangle \sim 0$ , which is consistent with the symmetric bicontinuous pattern evolution [see Fig. 2(b)]. For the mixtures of  $\beta \neq 0$ , on the other hand,  $\langle h \rangle$  increases till  $t \sim 150$  and then slowly decreases with time.

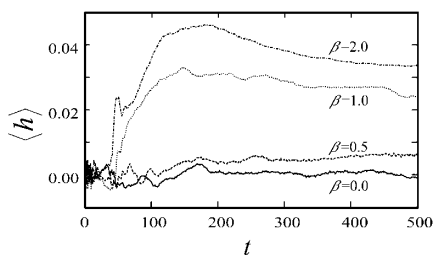


FIG. 3. Temporal change in the averaged curvature of the phase-separated interface of the fluid mixture for various  $\beta$ . Note that in the early stage ( $t \lesssim 50$ ), where a sharp interface is not yet formed, the averaged curvatures contain large errors.

The initial growth of  $\langle h \rangle$  reflects the morphological change of the domain pattern from the symmetric bicontinuous to the nematic droplet structure [see Fig. 2(c)]. On the other hand, its decay in the late stage simply reflects the domain coarsening. Note that  $\langle h \rangle$  is closely related to the characteristic domain size. Figure 3 shows that the deviation of  $\langle h \rangle$  from zero is larger for the mixture of larger  $\beta$ . We confirmed that the behavior for  $\beta < 0$  is essentially the same as that for  $\beta > 0$ . In other words, the nematic phase always tends to form isolated droplets, and not the matrix for a finite  $\beta$ , irrespective of the sign of  $\beta$ . We also confirmed that the anchoring effect does not play a role in the breakdown of the morphological symmetry; the same behavior is observed even for  $w = 0$ . These strongly suggest that the tendency of nematic droplet formation observed in Fig. 2(c) is due to the effects of the flow-alignment coupling, and not primarily due to the elastic effects.

Before discussing the mechanism, we point out that there can be the two types of spinodal decomposition for IL-LC mixtures, depending upon the quench condition. When a system is unstable solely against phase separation just after the quench, only phase separation proceeds initially and then it induces isotropic-nematic transition later [case (I) in Fig. 1]. We call this type “isotropic spinodal decomposition” (ISD). When a system is unstable against both phase separation and nematic ordering, on the other hand, nematic ordering takes place first and phase separation follows [case (N) in Fig. 1]. We call this type “nematic spinodal decomposition” (NSD). This retardation of phase separation reflects the faster kinetics of the nonconserved order parameter than the conserved one. Note that the orientational order parameter is non-conserved, while the composition one is conserved.

Figures 4(a) and 4(b) show the temporal change of the squared amplitudes of three relevant field variables,  $\Delta\phi^2$ ,  $Q^2$ , and  $|\vec{v}|^2$ , per lattice, together with the domain pattern (see the inset), respectively, for NSD and ISD.

For NSD [see Fig. 4(a)],  $Q^2$  develops faster than  $\Delta\phi^2$ . At  $t \approx 10$ , the IN transition is already finished and the entire system becomes the nematic state. Then this homogeneous nematic phase separates into the isotropic and nematic phases. The second increase of  $Q^2$  around  $t \approx 30$  reflects the increase of nematic order  $Q$  upon this phase separation and the resulting formation of the LC-rich phase. Reflecting this two-step ordering,  $|\vec{v}|^2$  has two peaks at  $t \approx 8$  and  $t \approx 30$ . The first peak is due to the flow induced by the coupling force between the director and flow field, that is,  $\beta\partial_j H_{ij}$  (the  $\mathbf{Q}-\vec{v}$  coupling). The second one, on the other hand, is due to the flow induced by the forces associated with the thermodynamic and deformation energy (the  $\phi-\mathbf{Q}$  coupling), that is,  $-\phi\partial_i\mu + \partial_j(H_{ik}Q_{kj} - Q_{ik}H_{kj}) + Q_{jk}\partial_i H_{kj}$ . For NSD, thus, the flow due to the  $\mathbf{Q}-\vec{v}$  coupling is completely decoupled from that due to the  $\phi-\mathbf{Q}$  coupling. For this case, the morphological symmetry is not broken [see the inset in Fig. 4(a)].

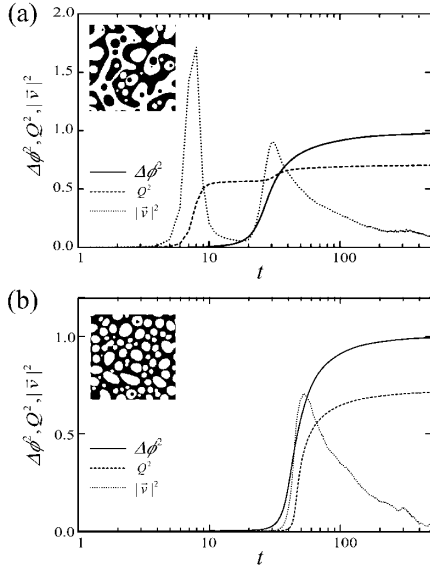


FIG. 4. Temporal change of the square of the field variables,  $\delta\phi^2$ ,  $Q^2$ , and  $|\vec{v}|^2$  for (a) NSD [case (N) in Fig. 1:  $\phi^* = -0.5$ ] and (b) ISD [case (I) in Fig. 1:  $\phi^* = 0.5$ ]. The other parameters are the same as those of Fig. 2(c). The domain patterns at  $t = 300$  are also drawn as the insets.

For ISD [see Fig. 4(b)], on the other hand, concentration fluctuations grow slightly before nematic ordering. The three field variables grow almost simultaneously, differently from the NSD case. The morphological symmetry is broken for this case [see the inset in Fig. 4(b)].

Now we are ready to answer how and why the morphological symmetry is broken by the flow-alignment coupling. In the initial stage, the flow field is induced by the formation of the domain interface and the resulting motion of it. This flow field aligns liquid crystal ( $\vec{v} \rightarrow \mathbf{Q}$ ), and this alignment motion further enhances the flow ( $\mathbf{Q} \rightarrow \vec{v}$ ). This positive feedback process, which is the result of the bidirectional coupling between  $\vec{v}$  and  $\mathbf{Q}$ , accelerates domain coarsening. The fact that this process exists only in the LC-rich phase leads to the breakdown of the morphological symmetry. Although the direction of the flow depends on the sign of  $\beta$ , its roles on the above mechanism, which is characterized by  $\beta^2$ , are the same. Thus, the degree of the breakdown of the morphological symmetry depends only upon the magnitude of  $\beta$ ,  $|\beta|$ . From our simulations, we learn that the occurrence of ISD and nonzero  $\beta$  are necessary conditions for the breakdown of the morphological symmetry. This can be explained as follows:  $\phi$  and  $\mathbf{Q}$  must develop almost simultaneously in the early stage. This is a necessary condition for the interface motion to be coupled to the orientational order via the above positive feedback mechanism. Furthermore, only when there is the coupling between  $\mathbf{Q}$  and  $\vec{v}$ , does the flow selectively coarsen the LC-rich domains via the flow-alignment coupling. Thus, we can conclude that the morphological symmetry breaking is the result of the strong cooperative couplings of the three relevant field variables,  $\phi$ ,  $\vec{v}$ , and  $\mathbf{Q}$ .

Finally, we stress that (i) LC is intrinsically an anisotropic fluid and the nematohydrodynamics always plays crucial roles in its dynamic behavior, and (ii) the  $\mathbf{Q}\text{-}\vec{v}$  coupling originates solely from the anisotropy of molecular shape and thus it is intrinsic to LC. These facts indicate that this morphological symmetry breaking and the resulting breakdown of the self-similar growth even for a symmetric mixture are intrinsic and generic to phase separation of IL and LC.

This work was partly supported by a Grant-in-Aid for Scientific Research from the Ministry of Education, Culture, Sports, Science and Technology, Japan.

- 
- [1] A. Onuki, *Phase Transition Dynamics* (Cambridge University Press, Cambridge, 2002).
  - [2] Morphological symmetry means that the topological characteristics of the structure is invariant under the exchange of the two phases.
  - [3] H. Tanaka, *J. Phys. Condens. Matter* **12**, R207 (2000).
  - [4] P. Palffy-Muhoray, J. J. de Bruyn, and D. A. Dunmur, *Mol. Cryst. Liq. Cryst.* **127**, 301 (1985).
  - [5] A. Ten Bosch, *J. Phys. II (France)* **1**, 949 (1991).
  - [6] C. Shen and T. Kyu, *J. Chem. Phys.* **102**, 556 (1995).
  - [7] Y. Lansac, F. Fried, and P. Maïssa, *Liq. Cryst.* **18**, 829 (1995).
  - [8] A. Matsuyama, R. M. L. Evans, and M. E. Cates, *Phys. Rev. E* **61**, 2977 (2000).
  - [9] D. Nwabunma, H.-W. Chiu, and T. Kyu, *J. Chem. Phys.* **113**, 6429 (2000).
  - [10] H.-W. Chiu and T. Kyu, *J. Chem. Phys.* **110**, 5998 (1999).
  - [11] R. Holyst and M. Schick, *J. Chem. Phys.* **96**, 721 (1992).
  - [12] A. J. Liu and G. H. Fredrickson, *Macromolecules* **26**, 2817 (1993).
  - [13] A. M. Lapeña *et al.*, *Phys. Rev. E* **60**, R29 (1999).
  - [14] J. Fukuda, *Phys. Rev. E* **59**, 3275 (1999).
  - [15] Here  $\mathbf{Q}(= Q_{ij})$  is defined as  $Q_{ij} = \frac{d}{d-1} Q(n_i n_j - \frac{1}{d} \delta_{ij})$ , where  $Q$ ,  $n_i$ , and  $d$  represent the degree of the orientational order, the normalized director field, and the dimensionality of the director field, respectively [16].
  - [16] P. G. de Gennes and J. Prost, *The Physics of Liquid Crystals* (Oxford, London, 1993), 2nd ed.
  - [17] P. D. Olmsted and P. M. Goldbart, *Phys. Rev. A* **46**, 4966 (1992).
  - [18] J. Fukuda, *Eur. Phys. J. B* **7**, 573 (1999).
  - [19] G. Tóth, C. Denniston, and J. M. Yeomans, *Phys. Rev. Lett.* **88**, 105504 (2002); D. Svehšek and S. Žumer, *Phys. Rev. E* **66**, 021712 (2002).
  - [20] H. Tanaka and T. Araki, *Phys. Rev. Lett.* **81**, 389 (1998).
  - [21] These parameters are estimated from the following typical values:  $\sigma \sim 5 \times 10^{-4}$  [N/m],  $K_F \sim 5 \times 10^{-12}$  [N],  $l \sim 1 \times 10^{-8}$  [m],  $\xi \sim 2.5 \times 10^{-8}$  [m], and  $\Xi \sim 1 \times 10^{-8}$  [m].
  - [22] Note that the similar morphological symmetry breaking can also be caused by the coupling between  $\phi$  and  $\mathbf{Q}$  in the free energy [10,13]. We stress that its physical origin is essentially different from ours. In our simulation, this effect is avoided by imposing the linear  $\phi$  dependence of  $a(\phi)$ .